

In-Flight Radiometric Performances Analysis of an Airborne Optical Payload

Caixia Gao, Chuanrong Li, Lingli Tang, Lingling Ma, Yaokai Liu, Xinhong Wang, Yongsheng Zhou

Abstract—Performances analysis of remote sensing sensor is required to pursue a range of scientific research and application objectives. Laboratory analysis of any remote sensing instrument is essential, but not sufficient to establish a valid inflight one. In this study, with the aid of the *in situ* measurements and corresponding image of three-gray scale permanent artificial target, the in-flight radiometric performances analyses (in-flight radiometric calibration, dynamic range and response linearity, signal-noise-ratio (SNR), radiometric resolution) of self-developed short-wave infrared (SWIR) camera are performed. To acquire the inflight calibration coefficients of the SWIR camera, the at-sensor radiances (L_t) for the artificial targets are firstly simulated with *in situ* measurements (atmosphere parameter and spectral reflectance of the target) and viewing geometries using MODTRAN model. With these radiances and the corresponding digital numbers (DN) in the image, a straight line with a formulation of $L = G \times DN + B$ is fitted by a minimization regression method, and the fitted coefficients, G and B, are inflight calibration coefficients. And then the high point (L_H) and the low point (L_L) of dynamic range can be described as $L_H = (G \times DN_H + B)$ and $L_L = B$, respectively, where DN_H is equal to $2^n - 1$ (n is the quantization number of the payload). Meanwhile, the sensor's response linearity (δ) is described as the correlation coefficient of the regressed line. The results show that the calibration coefficients (G and B) are $0.0083 \text{ W} \cdot \text{sr}^{-1} \cdot \text{m}^{-2} \cdot \mu\text{m}^{-1}$ and $-3.5 \text{ W} \cdot \text{sr}^{-1} \cdot \text{m}^{-2} \cdot \mu\text{m}^{-1}$; the low point of dynamic range is $-3.5 \text{ W} \cdot \text{sr}^{-1} \cdot \text{m}^{-2} \cdot \mu\text{m}^{-1}$ and the high point is $30.5 \text{ W} \cdot \text{sr}^{-1} \cdot \text{m}^{-2} \cdot \mu\text{m}^{-1}$; the response linearity is approximately 99%. Furthermore, a SNR normalization method is used to assess the sensor's SNR, and the normalized SNR is about 59.6 when the mean value of radiance is equal to $11.0 \text{ W} \cdot \text{sr}^{-1} \cdot \text{m}^{-2} \cdot \mu\text{m}^{-1}$; subsequently, the radiometric resolution is calculated about $0.1845 \text{ W} \cdot \text{sr}^{-1} \cdot \text{m}^{-2} \cdot \mu\text{m}^{-1}$. Moreover, in order to validate the result, a comparison of the measured radiance with a radiative-transfer-code-predicted over four portable artificial targets with reflectance of 20%, 30%, 40%, 50% respectively, is performed. It is noted that relative error for the calibration is within 6.6%.

Keywords—Calibration, dynamic range, radiometric resolution, SNR.

I. INTRODUCTION

AIRBORNE and spaceborne optical imaging sensors are essential in many environmental aspects, such as meteorology, surveillance, mapping, with spatial resolution ranging from several kilometers to several tens of centimeters. Their in-flight performances analyses are essential since the laboratory analysis is not sufficient to establish a valid inflight one. Since sensors cannot be directly tested in flight, it is still

Caixia Gao, Chuanrong Li, Lingli Tang, Lingling Ma, Yaokai Liu, Xinhong Wang, Yongsheng Zhou are now with Key Laboratory of Quantitative Remote Sensing Information Technology, Academy of Opto-Electronics, Chinese Academy of Sciences, Beijing, 100094, China (corresponding author: Caixia Gao; phone: 86-10-82178645; fax: 86-10-82178600; e-mail: gaocaixia@aoc.ac.cn).

the most common way to carry out these activities with the ground reference targets, and corresponding instruments. In view of this, great efforts have been dedicated to construct a comprehensive calibration and validation site in China, namely Baotou site supported by the National High-Tech Program of China. This site integrates most functions of aviation testing, in-flight calibration and performance assessment of remote sensing (RS) sensors and RS product validation [1]. In 2014, Baotou site was incorporated into the Radiometric Calibration Network of Automated Instruments (RadCalNet), with an aim of providing demonstrated global standard automated radiometric calibration service in cooperation with Europe Space Agency (ESA), National Aeronautics and Space Administration (NASA), the French National Space (CNES) and National Physical Laboratory (NPL). In this site, several permanent artificial targets were developed with the advantages of year-round availability, lower maintenance operations, long lifetime, and would be excellent references for airborne and spaceborne sensors. Thus, several campaigns were performed in Baotou site, and various RS sensors, including panchromatic, multispectral, hyperspectral, InSAR, etc., were tested. On October 17, 2014, a scientific experiment was orchestrated at the Baotou site to assess the performances of self-developed airborne optical payloads, and in this study radiometric performances (in-flight radiometric calibration, dynamic range and response linearity, signal-noise-ratio (SNR), radiometric resolution) of short-wave infrared (SWIR) sensor are given.

In this paper, Section II mainly gives the general description of Baotou site and flight campaign; Section III describes the methods and the corresponding results. Section IV gives a validation results with portal targets. Conclusions are drawn in Section V.

II. GENERAL DESCRIPTION OF BAOTOU SITE AND FLIGHT CAMPAIGN

A. General Description of Baotou Site

Baotou site is located in the Inner Mongolia, China, approximately 50 km away from Baotou city with convenient transportation. It covers a flat area of approximately 300 km^2 with an average altitude of 1270 m [1]. The site features a cold semi-arid climate, and is dominated by various land surfaces, including lake, sand, bare soil, maize, grass, sunflower, potato, pumpkin, etc., which can be used for quantitative remote sensing data and product validation. In addition, it is notable that several permanent targets, such as optical permanent artificial targets, bar-pattern permanent target, are installed in Baotou site. Among them, the knife-edge target with a size of $48 \text{ m} \times 48 \text{ m}$ and three scale (white scale, gray scale and black

scale) could be used for performing radiometric performances analysis and assess the Modulation Transfer Function (MTF) of optical sensors. The target was subordinated to RadCalNet for automated radiometric calibration in 2014, and meanwhile subordinated to United States Geological Survey (USGS) for MTF assessment. Under the framework of RadCalNet, three automated spectral reflectance measurement systems are developed, and are in operation for providing demonstrated global standard automated radiometric calibration service. The system is designed to observe ground every 10 minutes with a VIS-NIR spectrometer, and the surface reflectance at certain observing direction is calculated with hemispherical-conical reflectance and the Bidirectional Reflectance Distribution Function (BRDF) of the surface target.

Furthermore, large amount of instruments for measuring land surface, meteorological and atmospheric parameters are also equipped in Baotou site, such as SVC spectrometer, sun photometer Cimel CE318, automated weather station, meteorological sounding radar, etc. And Baotou site is also one of aerosol robotic network (AERONET) sites, which could provide globally distributed observations of spectral aerosol optical depth (AOD), inversion products, and total column water vapor (CWV) in diverse aerosol regimes.



Fig. 1 Worldview3 image over Baotou site on 27 Oct., 2015. (Band 5, 3, 2)

B. Flight Campaign

On October 17, 2014, a scientific flight campaign was orchestrated at the Baotou site to carry out inflight properties analysis of a self-developed airborne optical payload, whose spatial resolution is about 1.8m@1.5 Km. In this campaign, to investigate its radiometric performances, besides of the permanent knife-edge target, four portal gray-scale targets were laid out; meanwhile, the SVC spectrometer was used for measuring the target's spectral characteristics, and atmosphere characteristics, such as AOD, CWV, etc., were acquired by Cimel CE318 Sunphotometer and radiosonde (Fig. 2).

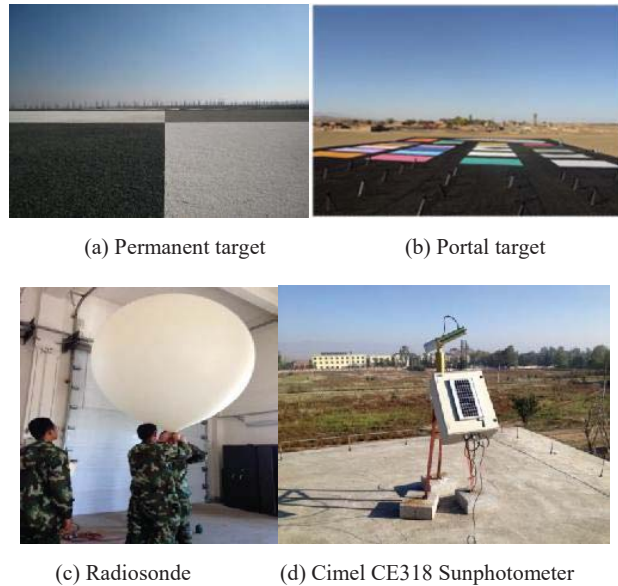


Fig. 2 Targets and instruments for performing radiometric performance of short-wave infrared sensor in this campaign

III. METHODS AND RESULTS

A. Radiometric Calibration

Analysis derived from data captured by multispectral sensors require previous knowledge of the radiometric calibration parameters of each channel. According to [2], radiometric calibration processes can be classified as laboratory calibration, onboard calibration, and vicarious calibration. Among them, vicarious calibration is an important way for airborne sensor calibration, which requires the target with uniform reflectivity with respect to the viewing direction and wavelength [3]. The artificial targets are more appropriate instead of nature scenes. In view of this, permanent knife-edge target with three scales were installed in Baotou site.

Vicarious calibration could be classified as reflectance-based calibration, irradiance-based method, and radiance-based method. In this study, reflectance-based calibration is used. With the aid of target reflectance and corresponding synchronous atmospheric parameters, the at-sensor radiance for each target is simulated using radiative transfer model—MODTRAN. Furthermore, the digital numbers (DN) of each target is extracted from the image, and then a regression line could be fitted between DN value and the at-sensor radiance. The simplified equation is defined as:

$$L = DN \times \text{Gain} + \text{Bias} \quad (1)$$

where L is the at-sensor radiance ($\text{W} \cdot \text{sr}^{-1} \cdot \text{m}^{-2} \cdot \mu\text{m}^{-1}$), Gain and Bias are calibration coefficients.

The flowchart of reflectance-based calibration method is shown in Fig. 3.

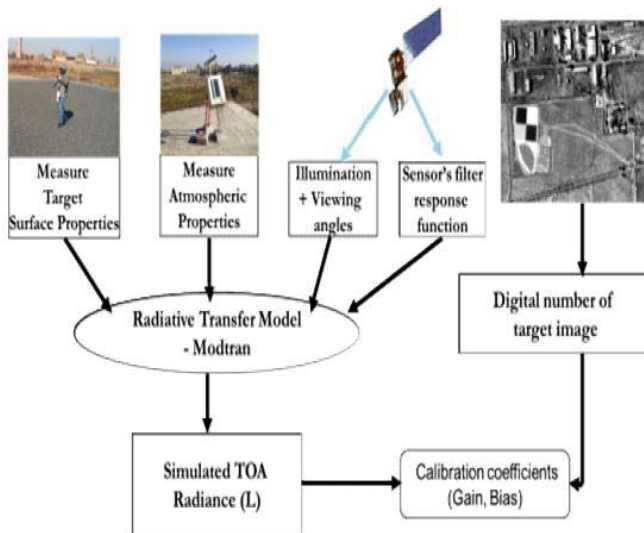


Fig. 3 Flowchart of radiometric calibration

With the aid of synchronous measurements of the knife-edge permanent target spectral reflectance (Fig. 4) and atmospheric parameters (AOD and CWV) on October 17, 2014, the calibration could be performed with the method described aforementioned. In this procedure, 10*10 pixels are selected around the center of each panel (white, black and gray panel) in SWIR image (Fig. 5), and the mean value of DN for these pixels is calculate. In Fig. 6, its calibration result is shown and it is noted that high correlation coefficient is presented.

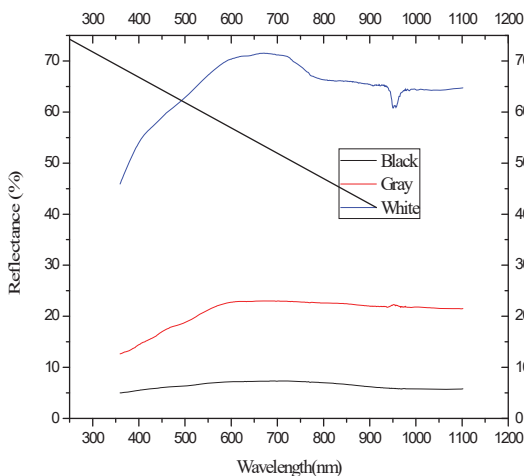


Fig. 4 Spectral reflectance of permanent target

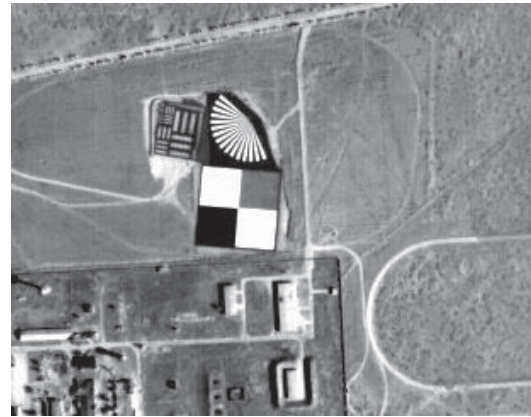


Fig. 5 SWIR image over Baotou site

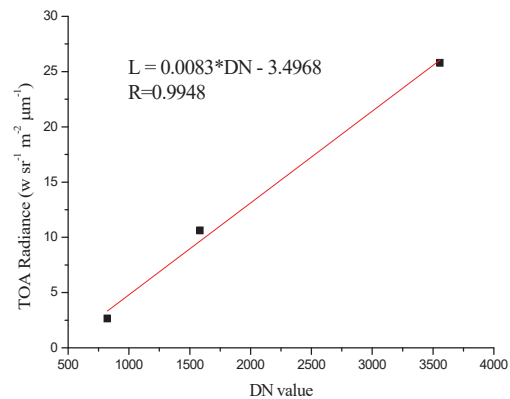


Fig. 6 Radiometric calibration result for SWIR airborne sensor

B. Dynamic Range and Response Linearity

Dynamic range impacts the brightness and contrast of the image, which is defined as the range of the maximal and minimal output of sensor [4]. In practice, it is difficult to assess it directly for the inflight sensors, thus, larger uniform target is required for its assessment indirectly. Similar to the procedure of radiometric calibration, the corresponding at-sensor radiance of each target is simulated with radiative transfer code MODTRAN, and then with the aid of the calibration coefficient, the high point (L_H) and the low point (L_L) of dynamic range could be described as $L_H = (G \times DN_H + B)$ and $L_L = B$, respectively, where DN_H is equal to $2^n - 1$ (n is the quantization number of the payload, $n=12$). And the coefficient of the regressed line is calculated, which is expressed as the sensor's response linearity (δ). Fig. 7 shows the illustration of calculating dynamic range. In this study, for the SWIR sensor, the calculated low point of dynamic range is $-3.5 \cdot W \cdot sr^{-1} m^{-2} \mu m^{-1}$ and the high point is $30.5 \cdot W \cdot sr^{-1} m^{-2} \mu m^{-1}$; the response linearity is approximately 99%.

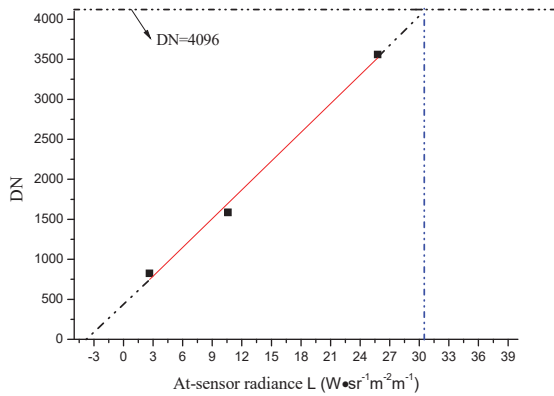


Fig. 7 The illustration of calculating dynamic range

C. SNR

SNR is usually considered as the ratio of average noise level to the average signal level for an image or for a sensor. It is noted that the SNR normalization method [5] could be better track these changes on sensor's SNR characteristics. In view of this, SNR normalization method is applied to the airborne SWIR image over permanent target because of its good homogeneity. In this method, three pixel blocks (black, grey and white blocks) are selected, and each block's SNR is calculated with the variance method, where SNR is calculated as the ratio of mean value to standard deviation for each pixel blocks. And then, with the SNR values for the three pixel blocks, the linear trend of SNR varying with at-sensor radiance could be estimated using least square method. Subsequently, the normalized SNR value is obtained according to the linear relationship between SNR and at-sensor radiance when the at-sensor radiance is assumed to be $11.0 \text{ W} \cdot \text{sr}^{-1} \text{m}^{-2} \mu\text{m}^{-1}$. The result is shown in Table I.

TABLE I
THE SNR ASSESSMENT RESULT

	Mean value of radiance ($\text{W} \cdot \text{sr}^{-1} \text{m}^{-2} \mu\text{m}^{-1}$)	SNR
Black block	3.64	55.3
Grey block	10.45	58.1
White block	26.54	75.5
Normalized to radiance=11.0	11.0	59.6

D. Radiometric Resolution

Radiometric resolution determines how finely a system can represent or distinguish differences of intensity. The higher the radiometric resolution, the better subtle differences of intensity or reflectivity can be represented, at least in theory [6]. In practice, the effective radiometric resolution is typically limited by the noise level, rather than by the bits number of representation. In the visible-near infrared spectral regions of the electromagnetic spectrum, radiometric resolution is represented by the noise equivalent reflectance ($\text{NE}\Delta\rho$) or the noise equivalent radiance ($\text{NE}\Delta L$). It is defined as the corresponding reflectance or radiance when the SNR of image is equal to 1. In this study, the radiometric resolution ($\text{NE}\Delta L$) is

acquired about $0.1845 \text{ W} \cdot \text{sr}^{-1} \text{m}^{-2} \mu\text{m}^{-1}$ using the SNR aforementioned and at-sensor radiance.

IV. VALIDATION

The simulated at-sensor radiance is major factor impacting the accuracy for SWIR radiometric performance assessment. In order to validate the result, four targets with surface reflectance of 20%, 30%, 40%, 50% respectively (Fig. 8) are used, and a comparison of the measured radiances with a radiative-transfer-code-predicted one over four portable artificial targets is performed. The measured at-sensor radiance is calculated from the calibration coefficient in Section III. It is noted that the relative error is within 6.6%.

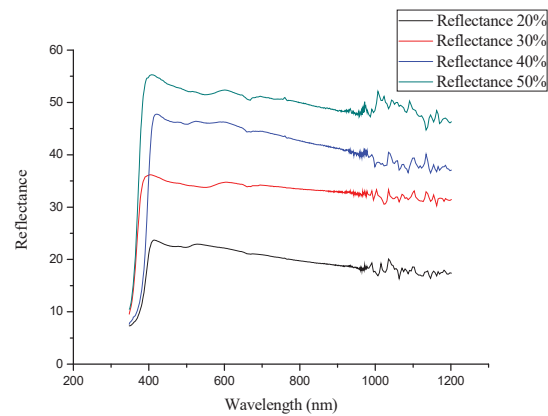


Fig. 8 Reflectance of portal gray-scale targets

TABLE II
VALIDATION RESULTS WITH PORTAL TARGETS

Reflectance of target	Measured radiance	Radiative-transfer-code-predicted radiance	Absolute error	Relative error
20%	7.966	8.497	0.531	6.6%
30%	14.021	14.869	0.848	6.0%
40%	16.88	16.952	0.072	0.43%
50%	20.991	19.770	-1.221	-5.8%

V. CONCLUSIONS

Baotou site is an excellent one for performing the performance assessment of optical and SAR sensors. In this study, a radiometric assessment, including radiometric calibration, dynamic range and response linearity, SNR, radiometric resolution, for the self-developed SWIR sensor is performed using the synchronous measurements in the large flight campaign. And it is worth noting that the radiometric calibration coefficient is $0.0083 \text{ W} \cdot \text{sr}^{-1} \text{m}^{-2} \mu\text{m}^{-1}$ and $-3.5 \text{ W} \cdot \text{sr}^{-1} \text{m}^{-2} \mu\text{m}^{-1}$; the dynamic range is $-3.5 \text{ W} \cdot \text{sr}^{-1} \text{m}^{-2} \mu\text{m}^{-1}$ to $30.5 \text{ W} \cdot \text{sr}^{-1} \text{m}^{-2} \mu\text{m}^{-1}$; the normalized SNR is about 59.6 when the mean value of radiance is equal to $11.0 \text{ W} \cdot \text{sr}^{-1} \text{m}^{-2} \mu\text{m}^{-1}$, and the radiometric resolution about $0.1845 \text{ W} \cdot \text{sr}^{-1} \text{m}^{-2} \mu\text{m}^{-1}$. And a validation is performed by comparing the measured radiance with a radiative-transfer-code-predicted over four portable artificial targets, and a relative error of 6.6% is presented.

ACKNOWLEDGMENT

The work has been supported by the National High Technology Research and Development Program of China 863 program (2013AA122102).

REFERENCES

- [1] C.R. Li, L.L. Tang, L.L. Ma, Y.S. Zhou, C.X. Gao, N. Wang, X.H. Li, X.H. Wang, and X.H. Zhu, "A comprehensive calibration and validation site for information remote sensing, Symposium on Remote Sensing of Environment," *Int. Symposium on Remote Sens. Environ.*, 11–15 May 2015, Berlin, Germany, Volume XL-7/W3, pp.1233-1240.
- [2] M. Dinguirard, and P.N. Slater, "Calibration of space-multispectral imaging sensors: A review." *Remote Sens. Environ.* 1999, vol.68, pp.194–205.
- [3] D. Susana, R. Pablo, H. David, and F. Beatriz, "Vicarious Radiometric Calibration of a Multispectral Camera on Board an Unmanned Aerial System," *Remote Sens.*, 2014, vol. 6, pp.1918-1937; doi:10.3390/rs6031918.
- [4] C. X. Gao, L.L. Ma, Y. K. Liu, N. Wang, Y.G. Qian, L.L. Tang, C.R. Li, "The assessment of in-flight dynamic range and response linearity of optical payloads onboard GF-1 satellite," *Proc. of SPIE*, 2014, Vol. 9264, doi:10.1117/12.2068794.
- [5] X.H. Wang, L.L. Tang, C.R. Li, B. Yuan, B. Zhu, "A practical SNR estimation scheme for remotely sensed optical imagery," *Proc. of SPIE*, 2009, Vol. 7384, pp. 738434-1–738434-6.
- [6] http://pgemejg.jottit.com/how_to_determine_image_resolution.